

2

NSWC TR 85-452

DTIC FILE COPY

AD-A183 642

**INFRARED EMISSION STUDY OF DEFORMATION
AND IGNITION OF ENERGETIC MATERIALS (IMAD
THE PROGRAM PROGRESS REPORT)**

BY P. J. MILLER C. S. COFFEY V. F. DeVOST

RESEARCH AND TECHNOLOGY DEPARTMENT

31 MAY 1986

DTIC
ELECTE
AUG 21 1987
S D

Approved for public release; distribution is unlimited.



NAVAL SURFACE WEAPONS CENTER

Dahlgren, Virginia 22448-5000 • Silver Spring, Maryland 20903-5000

UNCLASSIFIED

SECURITY CLASSIFICATION OF THIS PAGE

A.D. 83642

REPORT DOCUMENTATION PAGE

1a. REPORT SECURITY CLASSIFICATION UNCLASSIFIED			1b. RESTRICTIVE MARKINGS			
2a. SECURITY CLASSIFICATION AUTHORITY			3. DISTRIBUTION/AVAILABILITY OF REPORT Approved for public release; distribution is unlimited.			
2b. DECLASSIFICATION/DOWNGRADING SCHEDULE						
4. PERFORMING ORGANIZATION REPORT NUMBER(S) NSWC TR 85-452			5. MONITORING ORGANIZATION REPORT NUMBER(S)			
6a. NAME OF PERFORMING ORGANIZATION Naval Surface Weapons Center		6b. OFFICE SYMBOL (if applicable) R13	7a. NAME OF MONITORING ORGANIZATION			
6c. ADDRESS (City, State, and ZIP Code) 10901 New Hampshire Avenue Silver Spring, MD 20903-5000			7b. ADDRESS (City, State, and ZIP Code)			
8a. NAME OF FUNDING / SPONSORING ORGANIZATION Naval Sea Systems Command		8b. OFFICE SYMBOL (if applicable) SEA-64E	9. PROCUREMENT INSTRUMENT IDENTIFICATION NUMBER			
8c. ADDRESS (City, State, and ZIP Code) Washington, DC 20362			10. SOURCE OF FUNDING NUMBERS			
			PROGRAM ELEMENT NO. 63609N	PROJECT NO.	TASK NO. S0363	WORK UNIT ACCESSION NO. 20CB407
11. TITLE (Include Security Classification) Infrared Emission Study of Deformation and Ignition of Energetic Materials (IMAD HE Program Progress Report)						
12. PERSONAL AUTHOR(S) P. J. Miller, C. S. Coffey and V. F. DeVost						
13a. TYPE OF REPORT TR		13b. TIME COVERED FROM 6/85 TO 12/85		14. DATE OF REPORT (Year, Month, Day) 1986 May 31		15. PAGE COUNT 36
16. SUPPLEMENTARY NOTATION						
17. COSATI CODES			18. SUBJECT TERMS (Continue on reverse if necessary and identify by block number) Explosives Predictive Modeling Explosives Effects Insensitive Munitions Impact Sensitivity Detonation Physics			
FIELD	GROUP	SUB-GROUP				
19	04	01				
20	11	12				
19. ABSTRACT (Continue on reverse if necessary and identify by block number) Infrared measurements show that during rapid deformation of at least some crystalline and polymeric solids, heat is generated at unexpectedly high temperatures beginning essentially at the moment of deformation. The heat was observed by fast infrared sensors. Both the initial infrared emissions and the apparent blackbody temperatures were far in excess of what can reasonably be accounted for by the convention that distributes the energy due to deformation over the bulk of the solid. It appears that the origins of these high temperatures are associated with mechanical processes that effectively concentrate the energy of deformation into small local hot spot regions within the sample. These regions are most likely associated with shear bands and possibly fracture sites in the deforming crystal. (Key words)						
20. DISTRIBUTION/AVAILABILITY OF ABSTRACT <input checked="" type="checkbox"/> UNCLASSIFIED/UNLIMITED <input type="checkbox"/> SAME AS RPT <input type="checkbox"/> DTIC USERS			21. ABSTRACT SECURITY CLASSIFICATION UNCLASSIFIED			
22a. NAME OF RESPONSIBLE INDIVIDUAL P. J. MILLER			22b. TELEPHONE (Include Area Code) 202/394-2576		22c. OFFICE SYMBOL R13	

DD FORM 1473, 84 MAR

83 APR edition may be used until exhausted
All other editions are obsolete

SECURITY CLASSIFICATION OF THIS PAGE

★U.S. Government Printing Office: 1985-539-012

0102-LF-014-6602

UNCLASSIFIED

FOREWORD

This work was performed for and funded by the Explosives Advanced Development (EAD) Program, P.E. 63609N, Project No. S0363, the NAVSEA Explosives Development, Effects and Safety block program, SF33-337-691, and the NSWC Independent Research program office. The results and conclusions presented in this report concerning the formation and growth of hot spots should be of interest to those seeking explosive sensitivity to impact information and to those seeking a fundamental understanding and control of the mechanical deformation mechanisms involved in explosive initiation.

The authors wish to acknowledge the assistance of Drs. E. R. Lemar and J. W. Forbes for conducting the preliminary light gas experiments described in this report. On completion of these experiments, the results will be published in more detail.

Approved by:

Kurt F. Mueller

KURT F. MUELLER, Head
Energetic Materials Division

Accession For	
NTIS CRA&I	<input checked="" type="checkbox"/>
DTIC TAB	<input type="checkbox"/>
Unannounced	<input type="checkbox"/>
Justification	
By	
Distribution /	
Availability Codes	
Dist	Avail and/or Special
A-1	



CONTENTS

<u>Chapter</u>		<u>Page</u>
1	BACKGROUND	1
2	EVALUATION OBJECTIVES	2
3	EXPERIMENTAL APPARATUS	3
	DETECTION APPARATUS	3
	DROP TEST APPARATUS	3
	GAS GUN APPARATUS	4
4	IR EMISSION DATA ANALYSIS	5
5	EXPERIMENTS	7
	IMPACT EXPERIMENTS	7
	PRELIMINARY GAS GUN EXPERIMENTS	8
6	CHARACTERIZATION OF EXPLOSIVE SENSITIVITY AND RATE OF REACTION	11
	DISCUSSION OF EXPERIMENT RESULTS	11
	USEFULNESS FOR PREDICTIVE MODELING AND TESTING FOR SAFETY AND VULNERABILITY	12
7	SUMMARY OF RESULTS	14
	REFERENCES	30
	DISTRIBUTION	(1)

ILLUSTRATIONS

<u>Figure</u>		<u>Page</u>
1	APPARATUS USED FOR DETECTING IR EMISSION	15
2	SCHEMATIC DRAWING OF ANVIL AND OPTICAL COMPONENTS	16
3	IMPACT MACHINE	17
4	DROP TEST ANVIL	18
5	SCHEMATIC DIAGRAM OF GAS GUN EXPERIMENTAL CHAMBER	19

ILLUSTRATIONS (Cont.)

<u>Figure</u>		<u>Page</u>
6	INFRARED EMISSION DATA AND TWO-COLOR TEMPERATURE OF NaCl DUE TO 18.5 m/sec IMPACT	20
7	INFRARED EMISSION DATA AND TWO-COLOR TEMPERATURE OF AP DUE TO 18.5 m/sec IMPACT	21
8	INFRARED EMISSION (A) AND ACCELEROMETER RESPONSE (B) OF RDX IMPACTED WITH 5.5 m/sec VELOCITY	22
9	INFRARED EMISSION (A) AND ACCELEROMETER RESPONSE (B) OF PETN IMPACTED WITH 5.5 m/sec VELOCITY	23
10	PBXN-103 IMPACTED AT 19 m/sec. IR RESPONSE AND CALCULATED (IGNITION) TEMPERATURES	24
11	INFRARED EMISSION (A) $>5.5 \mu\text{m}$ and (B) $<5.5 \mu\text{m}$ AND CALCULATED TWO-COLOR TEMPERATURE (C) OF SINGLE CRYSTAL NaCl IMPACTED AT 485 m/sec	25
12	INFRARED EMISSION (A) $>5.5 \mu\text{m}$ and (B) $<5.5 \mu\text{m}$ AND CALCULATED TWO-COLOR TEMPERATURE (C) OF PETN SINGLE CRYSTAL SANDWICHED BETWEEN TWO NaCl CRYSTALS	26
13	AMMONIUM PERCHLORATE IGNITED AT 18 m/sec IMPACT	27
14	INFRARED EMISSION DATA FROM A SERIES OF PBX'S IMPACTED AT 17.5 m/sec ON SAND	28

TABLES

<u>Table</u>		<u>Page</u>
1	COMPARISON OF IR EMISSION RATES AND ESTIMATED REACTION RATES FOR SEVERAL EXPLOSIVES	29

CHAPTER 1

BACKGROUND

Time-resolved temperature measurements of shocked non-energetic materials by infrared radiometry in the low pressure range have become experimentally feasible, and brightness^{1,2} and two-color^{3,4} temperatures of shocked materials have been reported. In addition, reports^{5,6} describing the use of this technique to investigate reactive shocks in explosive materials to provide a new and versatile diagnostic tool in the study of initiation and build-up to detonation have also been published. These latter experiments resulted in the first direct measurement of the temperature of hot spots resulting from shock induced heating in explosives. In studies of shocked nitromethane, these results clearly indicated that a partial shock-induced chemical reaction took place before detonation.

Impact testing equipment in current use and new impact monitoring instrumentation were recently evaluated.⁷ Results of the evaluation showed that there are significant differences in the response of different tools used to impact explosives and of test samples having different geometries. The results of that study showed that transducers and IR sensors can be used effectively to monitor deformation, heat emission and reaction of explosive test samples during low velocity mechanical impact.

Here, we will present an investigation of the technique of measuring impact-induced time-resolved infrared emission as a diagnostic tool in studying deformation and initiation, deflagration, and build up to detonation in energetic materials for use with mechanical impact testing apparatus.

CHAPTER 2
EVALUATION OBJECTIVES

An investigation of the time-resolved IR emission technique was undertaken to achieve the following objectives:

- a. To determine the correlations between the infrared response and the pressure-time history of the mechanical impact; i.e., the dependence on pressure amplitude, on pressure rate of increase, and on deformation rate.
- b. To determine the rate of chemical reactivity of test samples undergoing mechanical impact with respect to the parameters described in a.
- c. To determine the accuracy of the time resolution and temperature derived data.
- d. And, to explore means of improving and extending these kinds of measurements on low velocity mechanical impacts on explosives under confined conditions, so that correlations between small-scale and large-scale testing can be obtained.

CHAPTER 3

EXPERIMENTAL APPARATUS

Detection Apparatus

A photograph of the basic apparatus used for measuring the deformation-induced infrared emission is shown in Figure 1; the schematic drawing showing specific details is shown in Figure 2. The two detectors were purchased from New England Research Center, Inc. They have HgCdTe detector elements. Also, InSb detectors were purchased from Barnes Engineering, Inc. and were used in some experiments. In order to insure fast response times of less than 10 nanoseconds, the detectors were operated in the photovoltaic mode rather than the conventional photoconductive mode. Also the size of the detector elements was kept to a maximum of a 0.2 mm x 0.2 mm square area. This latter requirement, unfortunately reduced the detectivity, D^* , of the detectors, but not to the point where they were not sufficiently sensitive. The cutoff wavelength for these detectors was approximately 13 microns (850 cm^{-1}). The detector response peaked at 11 microns (900 cm^{-1}) and extended into the near IR to about 1 micron ($10,000 \text{ cm}^{-1}$).

Two wideband pre-amplifiers were purchased to amplify the detector signals. Their important specifications were:

Gain.	26 DB
Bandwidth.	1 KHz -100 MHz
Pulse response.	4 nanoseconds

The pre-amps were operated under non-bias voltage conditions.

The remainder of the detection apparatus consisted of various types of beam splitters (both dichroic and achroic), dichroic filters, and lenses (BaF_2 , cutoff frequency 13 microns/ 850 cm^{-1} and silicon, cutoff frequency in the far infrared). These along with the detectors were assembled in an apparatus, shown in Figures 1 and 2. The specific optical arrangement for each experiment described in this report will be shown in the later sections of this report.

Drop Test Apparatus

Updating of small-scale and other low velocity shock tests in support of explosive physics research at NSWC has been in progress for the past few years. A nonstandard test using a portable experimental machine that is designed to quantify impact loading and explosive sample responses has been described.

The impact machine currently being used for the tests described in this report is a converted WOX 126A Drop Shock Test Set. This seven-foot tall, portable machine was formerly used to screen electronic components for shock hardness. A portable machine was selected to make it possible to share in-place instrumentation and existing laboratory spaces. Conversion of the machine consisted of replacing the test carriage with interchangeable drop weights and the shock pads with instrumented anvils. A release mechanism was added to the machine to provide remote operation, and shock cord accelerators (slings) were installed to increase its 1.5 meter drop height capability to an equivalent free-fall drop height of approximately 20 meters when accelerating a 0.5 kg drop weight. The machine is shown in Figure 3.

The anvil, shown in Figure 4, consists of a sapphire cylinder 1.905 cm in diameter by 1.25 cm high. This was cut from a single crystal with the ends polished to optical flatness. The sapphire anvil transmits both visible and infrared emissions out to wavelengths of approximately 6.5 microns. For longer wavelengths silicon or germanium anvils were used.

Gas Gun Apparatus

The apparatus used to carry out the high-velocity shock wave experiments in order to evaluate the time-resolved IR emission technique is the NSWC/WO Light Gas Gun. The explosive facility of NSWC/WO contains a single stage light gas gun and, in addition, has various methods of using high explosives to drive shock wave experiments. The light gas gun has a bore of 89 mm and is capable of driving projectiles at velocities from 0.1 to 0.8 km/sec. It was installed with its muzzle in an explosive test chamber (bombproof) so that targets may include very reactive materials. Up to 2.3 kg of explosive can be used in the test chamber for a single experiment. The gun is used to drive dynamic high pressure experiments in which the targets may be made of reactive materials (explosives or propellants) or inert materials. The facility is primarily used to obtain the equations of state of inert materials and of explosives in the unreacted state, and to measure shock wave evolution within these materials.

In the present experiments, the test chamber arrangement, as shown in Figure 5 was aligned with a helium-neon alignment laser positioned at the breech of the gun. The detection apparatus arranged in the test chamber at the muzzle of the gun had the same optical configuration as for the drop weight experiments. The projectile was designed such that a thin copper flyer plate with a velocity of ~485 m/sec impacted a NaCl single crystal sample (37.5 mm diameter and 6.5 mm thick) parallel to its (001) principal axis. The known Hugoniot parameters of the materials allowed for a calculation of 29 kbars \pm 5% initial pressure on the NaCl sample. The estimated accuracy in determining the arrival of the shock wave at the sample and the emergence of the wave at the rear of the sample is \pm 50 nsec. The NaCl crystal faces were flat to less than a $1/10\lambda$ at 6000Å and were parallel to less than 30 seconds.

CHAPTER 4

IR EMISSION DATA ANALYSIS

The response of a detector to black body emission may simply be described by

$$W_{\Delta\lambda}^{\text{obs}} = G \int_{\Delta\lambda} e(\lambda) W^{\text{bb}}(\lambda, T) d\lambda ,$$

where T and λ are temperature and wavelength and W^{obs} is the observed radiance from the wavelength interval, $\Delta\lambda$, obtained from the voltage response of the detector; G is a constant optical geometrical factor representing the light-gathering capability of the optics, $e(\lambda)$ is the emittance, and $W^{\text{bb}}(\lambda, T)$ is a black body function with the detector responsivity and optical component wavelength dependence incorporated into it.

A brightness temperature for any given experiment may be obtained by calibrating a single detector with a known black body source, as long as G remains constant; and, of course, if $e(\lambda)$, the emittance is assumed to be the same for both the black body source and the sample in question, and also if it is assumed that the sample emits black or grey body radiation. By simultaneously measuring the emission at two different wavelength intervals, a two-color temperature may be determined. This derived temperature represents an estimate of the true temperature, independent of $e(\lambda)$, provided that $e(\Delta\lambda_1) = e(\Delta\lambda_2)$, and provided that the emitted radiation follows a black body function. With the above assumptions, it is possible to evaluate $e(\lambda)$ by comparing the brightness temperature and the two-color temperature. The quantity $e(\lambda)$ is a direct measurement, then, of the fraction of the surface of the sample, as seen by the detector, which is hotter than the surrounding material. Thus this quantity represents the fraction reacted or the hot portion of the sample being observed. In the impact and shock experiments described here, this becomes an important quantity because the origin of the induced observed emission relates directly to the mechanism for hot spot formation and growth.

The errors from the temperature measurements, as described here, arise from two main sources: first, experimental error can result from the non-reproducibility of optical alignment between the calibration and sample runs and also from the signal to noise levels of the observed signals; second, error can arise from the assumptions being used in the black body model. For example, in the brightness temperature determination, if the sample acts like a grey body with $e(\lambda)$ less than 1.0, the observed temperature will be a lower limit, or will be less than the true temperature. In the two-color temperature, $e(\Delta\lambda_1) = e(\Delta\lambda_2)$ is generally a good approximation and the observed temperature is a true estimate of the actual temperature. When comparing the brightness temperature to the two-color temperature for a given

experiment the fraction of sample hot or reacted, $e(\lambda)$, also represents a lower limit to the true fraction of sample surface heating. Furthermore, a very important factor that can cause error will be the deviation from black body behavior that results from selective molecular emission.

CHAPTER 5
EXPERIMENTS

Impact Experiments

As described previously, two sets of experiments were performed to evaluate this technique for investigating the deformation induced heating in two different loading rate regimes. For low loading rates, the impact machine was used. Here the signals from each detector were passed through fast, broad band amplifiers and recorded simultaneously on dual beam digital oscilloscopes (0.5 μ sec response). Also recorded simultaneously on a separate dual beam oscilloscope were signals from an accelerometer and one of the infrared detectors. The accelerometer was mounted on the dropweight 3.57 cm from the impact surface and was used to monitor the deceleration of the drop weight during impact. Because of the distance between the accelerometer and the hardened steel (Rockwell 62) impacting surface of the drop weight, the accelerometer signal was delayed 6.5 μ sec from the infrared signal. The time resolution of the experiment was limited by the response of the accelerometer which was measured to be approximately 1 μ sec.

Both before and after a series of impact experiments the infrared detectors were calibrated with a black body source and mechanical chopper wheel placed against the sapphire anvil in approximately the same position as the material to be impacted. The calibration of the accelerometer was regularly checked throughout the duration of the experiments. Impact experiments were conducted on NaCl, NH_4ClO_4 , RDX, PETN, and PBXN-103, as well as several composite materials. The NaCl, NH_4ClO_4 , RDX and PETN samples were single crystals approximately 1.5 mm on a side and with masses of about 30-50 mg. The PBXN-103 samples were in the form of pellets with masses of ~35mg. NH_4ClO_4 , RDX and PETN are energetic materials which can react violently under impact of sufficient severity. In those cases where rapid reaction occurred the resulting infrared emissions were very different from those from the unreacted samples. In those cases where rapid reaction did not occur the observed emissions from the energetic materials and the inert materials were essentially the same.

Figures 6, 7, 8, and 9 show the recorded infrared data of impacts of single crystals of NaCl, NH_4ClO_4 , RDX and PETN respectively. Figure 10 shows similar data from an impact on a disk of PBXN-103 explosive. In these experiments, as in all that we have done to date, the infrared emissions appear essentially simultaneous with the first indication of deceleration. Of particular significance is the fact that the initially observed detector responses correspond to heating far above the 30°C threshold of the detection apparatus estimated for this optical arrangement. For the RDX example, the change in velocity of the drop weight in the first 15 μ sec after impact is approximately, $\Delta v = 2 \times 10^{-3}$ m/sec. The change in kinetic energy of the drop

weight is

$$\Delta U = mV_0 \Delta v$$

with $V_0 = 5.54$ m/sec and $m = 0.5$ kg so that $\Delta U = 5.5 \times 10^{-3}$ J. If all of this energy were distributed over the bulk of the crystal, the temperature increase would be $\Delta T \sim \frac{\Delta U}{\rho C_v} = 0.2^\circ\text{C}$, where $C_v = 0.3$ cal/gm $^\circ\text{K}$ and ρ , the mass, is 21

mg. This temperature is far below the typically estimated initial temperatures of 200°C observed in most of these experiments at 15 μsec after impact. This temperature is, also, far below the threshold detection level of the detectors involved. This result indicates that the energy of deformation is being localized, producing the observed high temperatures. Using the calculated 0.2°C rise in temperature due to the kinetic energy transfer, it can be estimated, that this energy must be localized in a volume of 1/200 of the sample to reach the detection limit of the detectors. To achieve the temperatures of 200°C , measured here, the local volume would have to be of the order of 1/1000 of the volume of the initial impacted sample.

Preliminary Gas Gun Experiments

In the drop weight experiments the initial temperatures estimated were above 200°C . In none of these experiments was the buildup to this temperature observed, for two reasons: first, the resolution of the digital oscilloscope used is limited to 0.5 μsec per data point and probably the temperature buildup occurs within this time frame; second, the fraction of sample surface that is being heated in the low velocity impact is too small to allow for enough radiation with sufficient signal-to-noise ratio to reach the detectors in the initial stages of sample deformation for detection.

In the preliminary gas gun experiments (to be published when the work is completed), the certainty in the measured arrival of the shock wave entry into the NaCl sample is of the order of 50 nsec and the detector signals are recorded with an analog oscilloscope with time resolution of a few nanoseconds. Here, the sample size was 37 mm dia x 6 mm and because of the 485 m/sec velocity and the ~ 30 kbar initial shock pressure in the NaCl sample, more than sufficient signal was observed to see the initial buildup of temperature due to the shock induced deformation. Figure 11 shows the recorded infrared emission from a single crystal of NaCl and its two-color temperature profile. The experimental set up for this experiment is shown in Figure 5. The signal-to-noise ratio of the observed detector signals is sufficient to show that infrared emission occurs within 25 nanoseconds of the estimated time of arrival of the shock front at the sample surface. The amplitude of the observed infrared signals and the ratio of signals (related to temperature increase) both appear to increase exponentially with time. The estimated temperature profile ranges between $\sim 40^\circ\text{C}$ and $\sim 650^\circ\text{C}$ with 200°C being reached within one μsec after the shock enters the sample. Unfortunately, the maximum temperature reached was not recorded as the observed signals increased beyond the voltage setting of the oscilloscope.

In the second gas gun experiment, a target sample was prepared by sandwiching a single crystal of PETN (2 cm x 2 cm x 0.4 cm) between two NaCl

crystal plates (3.7 cm dia. x 0.65 cm) as shown in Figure 5. The same projectile velocity and shock conditions were used for this shot as in the previous experiment. Since the image of the PETN crystal did not fill the detector area, radiation from the front NaCl plate also reached the detector. NaCl is infrared transparent in the spectral regions seen by the detectors, while PETN is not transparent, thus radiation that emits from the PETN would only be observed when the shock front reaches the rear of the PETN crystal. In fact this was observed. Figure 12 containing the detector responses shows very clearly that the observed infrared response profile matches that of the entry and exit of the shock front with the interfaces of the sandwich sample. The arrows on the figures represent the calculated points in time. Very satisfying is the fact that the temperature profile of this shot duplicates the previous shot where the shock front passes through the first NaCl window. The temperature here rises to just above 600°C; also, it appears that under these experimental conditions that this is a limiting temperature. When the shock enters the rear NaCl plate of the sample a further increase in temperature is observed in the figure, presumably this is due to an increased temperature that is radiating at the PETN face. Here again, the maximum temperatures were not observed because the oscilloscope was set at too sensitive an amplification (although it was set at a 5x less sensitive position than the previous shot).

Under these shock conditions, using a Gruneisen equation of state, and considering only the bulk properties of the material, it can be calculated that NaCl should only reach a temperature of approximately 200°C. The estimated temperatures in these experiments, if they are correct, indicate directly the localization of energy in the NaCl into hot zones or "spots". Considering the enormity of the detector signals in the gas gun shots as compared to the drop test runs, it is difficult not to believe that temperatures considerably greater than 200°C were achieved. In fact, it would perhaps be reasonable to believe that the limiting temperature rise is the melting point of NaCl at 801°C, since if extreme localization of energy did occur the melting process would absorb most of the excess energy. The observed lower 600°C - 650°C could be a result of calibration errors or could be a result of observing a distribution of temperatures giving an average somewhat lower than the maximum 801°C.

These tests were repeated with a copper plate attached directly to the back of the NaCl, in addition the edges of the NaCl sample were masked off with a central mask diameter opening of one inch. The resulting IR emission signals were extremely weak, less than 2 mv in amplitude. A second shot was then prepared where now the center of the sample was masked off with a 1" diameter mask. This NaCl sample also had a thin copper plate attached to the front surface. The shot was repeated and a substantial IR emission signal was then recorded, of 10-15 mv in amplitude.

Thus, the results of these experiments, indicate that the observed infrared emissions, which result from heating, occur in the shear and fracture at the edges of the sample where the reflected, rarefactions of the shock wave break up the sample. Very little IR emission occurs from the center of the sample only bulk compression occurs. This result is consistent with current theory for the formation of hot spots and explosive initiation for both heterogeneous and homogeneous explosives. The center of the NaCl sample

behaves homogeneously in that the heating is apparently due to bulk compression effects whereas the edges of the sample behave heterogeneously due to the irregularities of the mass flow of the sample breakup. An interesting and planned experiment will be to repeat these experiments on large single crystals of PETN and to look at the observed surface heating with an array detector which can measure the spacial emittance in the infrared. If PETN behaves as NaCl, one should see bulk heating from the center of the sample and the formation of hotspots on its edges.

Von Holle⁸ reported similar results on polymethylmethacrylate (PMMA) and polycrystalline KBr. The PMMA results indicated that the intense emitted radiation at the interface resulted from damage at the projectile-PMMA interface and that this could be sharply reduced by applying a thin film of silicon oil at the interface. However, the explanation for the large signals observed from the pressed polycrystalline KBr samples was that the emission occurred from impurities situated near inhomogeneties which were heated to higher temperatures than the bulk KBr. This is in contrast to the results offered in this study which seem to indicate that the observed large emissions occurs within the localized areas of the sample itself where the shear is large.

Other alternative explanations have been put forward to explain the observed large infrared emissions. Since the front of the NaCl crystals were transparent, what is observed are emissions from nitrogen ionizing in the air present in the test chamber (~10 torr) between the flyer plate and NaCl at impact. However, when air molecules ionize, they generally emit at selective wavelengths in the visible and uv spectrum. In the infrared this also would be at selective wavelengths and radiation would not be expected to last the lifetime of these experiments, 2-6 μ sec. Another explanation for the observed signals would be the result of impurities, such as H₂O, or other imperfections, in the NaCl crystal lattice that under shock result in various types of unstable electron centers being formed which result in emitted radiation. However, here again, these kinds of centers generally emit radiation from electronic transitions at selective uv-visible wavelengths. This is also true for infrared emission of molecular impurities if they occur. Although it can't be proven by these experiments, the observed infrared emissions appears to be broad band, since results from the low velocity experiments for four different wavelength intervals give similar results. Neither of the above alternative explanations for the observations of these present experiments appear to be justifiable.

CHAPTER 6

CHARACTERIZATION OF EXPLOSIVE SENSITIVITY AND RATE OF REACTION

Preliminary tests were performed to determine the applicability of this technique for the small scale characterization of explosive sensitivity and explosive vulnerability, and safety. This section will describe the results of these early tests and may possibly demonstrate the utility of this technique for small scale quantitative predictive testing and modeling of explosive sensitivity, vulnerability, and safety.

Discussion of Experiment Results

Figure 13 shows typical curves obtained from these types of experiments. This example, of single crystal of AP impacted at 17.5 m/sec with a 1/2 Kg weight, will be used to discuss descriptively the events that take place in an energetic material when impact initiation occurs and the utility of this method for predictive testing and modeling. In the figure, the response of the IR detectors in the first 50 μ sec is typical of what is observed for inert single crystal materials. The calculated two-color temperatures show an initial high temperature that decays in time and then increases at a later time near the end of the recorded event. The mechanism by which this occurs is at present under intense theoretical, and experimental investigation for this is a key to understanding mechanical initiation of explosives. At present, it is believed that the initial heating occurs instantaneously with deformation.

It is believed that localized heating, i.e. hot spots, occurs in the induced cleavage and slip planes of the fractured materials. From gas gun experiments, these temperatures peak within 2-3 μ secs with the melting point as the limiting temperature for inert materials. For the drop weight experiments, the stress of the deformation is relieved by the formation and propagation of induced cracks and fractures (an individual fracture propagates at near the sound velocity in the material). Finally, the drop weight catches up to the fractured material and induces a further deformation, thus an additional rise in temperature of the impacted material occurs through a similar mechanism. Controlled experiments on single crystals have shown that the induced slip planes and cleavage planes occur within the first 10 microns of deformation and that after only \sim 100 microns of deformation, the crystals are broken into many fine particles of a few microns in size. For energetic single crystal materials, explosive initiation depending on the rate of deformation, can occur at the initial deformation or, as seen in Figure 13, at the final deformation when the drop weight stops. In experiments using powdered composite explosives, the initial heating of fine bonded particles, such as RDX and HMX, is obscured; only the heat of initiation is picked up by the detectors.

When initiation takes place the IR emission response increases dramatically, as shown in Figure 13. The amplitude and the rate of increase in the amplitude of this signal depends only on two factors: the distribution of hot spots formed in time during the impact and on their rate of growth and decay. Under these non-shock conditions, the rate of growth of a single hot spot will specifically be characteristic of a material, statistically varying primarily due to the heterogeneity of the material and not specifically dependent on the nature of the stimulus that caused the formation of that hotspot. The distribution and formation of hotspots, however, will depend directly on the nature of the given stimulus and the response of the material to it. This will also be a statistically varying number depending on how homogeneous the material being investigated is and how the stimulus varies from drop to drop. As a consequence of the possible variations in the formation and growth of hot spots, the probability that ignition occurs will display a similar wide range of threshold values for a given stimuli. This has been found to be true for both the small scale mechanical impact tests as well as the large scale vulnerability and safety tests (bullet, multi-fragment, and sympathetic detonation). Thus, the specific tests, either small scale or large scale, must be defined in terms of probabilities of an event occurring and sufficient data will be required in order that statistically meaningful results may be obtained.

At this point, without further quantitative understanding, for a given specific mechanical stimulus, such as a drop weight test with fixed drop weight mass and velocity, anvil materials, size, shape and form of explosives, a qualitative ranking for explosives may be obtained for sensitivity and violence of reaction. Since the IR emission reveals at what time after impact the initiation threshold (or hot spot density threshold) occurs and the accelerometer gives the change of velocity of the drop weight during this time, a specific energy for initiation can be calculated. This value represents, for a given test, the amount of energy necessary for initiation which in turn represents the sensitivity of the explosive. Experiments have shown that for a given drop weight test there can be as much as 2 orders of magnitude difference between PBXN-103 and PBXW-109(Q). In ranking the explosives according to their reaction rate (or violence) to the given test, the slopes of the emission curves which represent the rate of sample consumption (hot spot growth) are compared. Here, again there are 2-3 orders of magnitude differences between PBXN-103, PBXW-115(Q), H6, PBXW-109(Q) and PBXN-106 for a given test Table 1. (IR Emission data shown in Figure 14).

We have not conducted enough tests at other impact levels and with different stimuli to determine whether the ranking order we show could change (tests have been conducted at two velocities, 5.5 and 17 m/sec). Thus far, only PBXN-103 has been tested enough times to obtain statistical information; the results showed at least a $\pm 30\%$ variation in the response of the materials.

Usefulness for Predictive Modeling and Testing for Safety and Vulnerability

It is one thing to describe a small scale test and to show how strongly the results are dependent on test conditions and it is another to attempt to relate these tests to large scale generic conditions for predictive capabilities. From this investigator's point of view in order to predictively model the effects of bullet, fragment, and sympathetic detonation on munitions

containing PBX's, three types of probability information will be needed: first, it will be necessary to know the extent of explosive deformation that occurs from the given stimulus; second, it will be necessary to know for a given deformation to what extent hot spots are formed; and third, it will be necessary to know what threshold of hot spot density will cause a sustained growth rate to produce burn, deflagration, or detonation.

The ultimate goal of the small scale tests described here is to determine the probability that an impact or shock induced deformation will cause initiation. This information, if introduced into a hydro-code calculation of explosive deformation by shock or impact, should make it possible to predict the probable violence of its response.

CHAPTER 7

SUMMARY OF RESULTS

The results of this study clearly indicate that the use of time-resolved infrared radiometry is a viable diagnostic tool for the investigation of rapid deformation effects on energetic materials. The data presented demonstrates a definite correlation between the pressure-time profile and the infrared emission-time profile of impacted materials. This technique can indeed be used to probe the heat development and its distribution in materials under deformation and can be used in the elucidation of the mechanisms involved in such predetonation phenomena.

The results reveal that infrared emission can be observed to occur in all materials under impact in a drop weight apparatus to within a few microseconds after impact. The observed time resolution is limited only by the timing devices of the apparatus and the amplitude of the signals. In the gas gun experiments, the emission is observed to occur within nanoseconds. The results of this study also show, that by using a model for black body radiation, two-color temperature-time profiles may be obtained from the experimental data with a good degree of precision. Further, it is possible to determine, with the model, some knowledge about the fraction of sample emitting heat during deformation.

The determination of temperature and of fraction of sample reacted depends on the black body assumption. A series of experiments are planned in the near future to verify this assumption. An infrared array detector will be used to measure the spectrum of the emitted radiation and to measure the spatial evolution of heat from the sample volume.

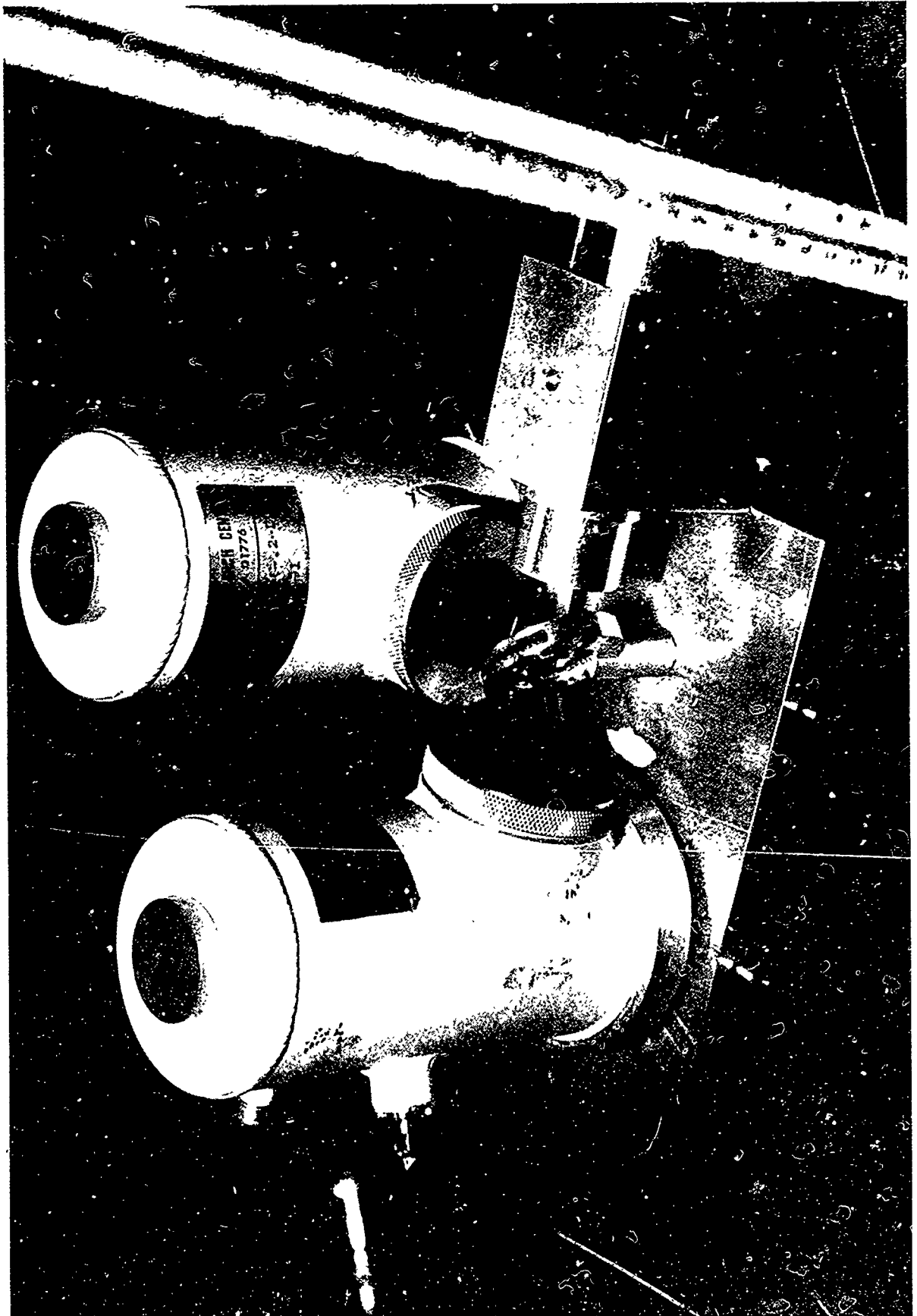


FIGURE 1. APPARATUS USED FOR DETECTING IR EMISSION

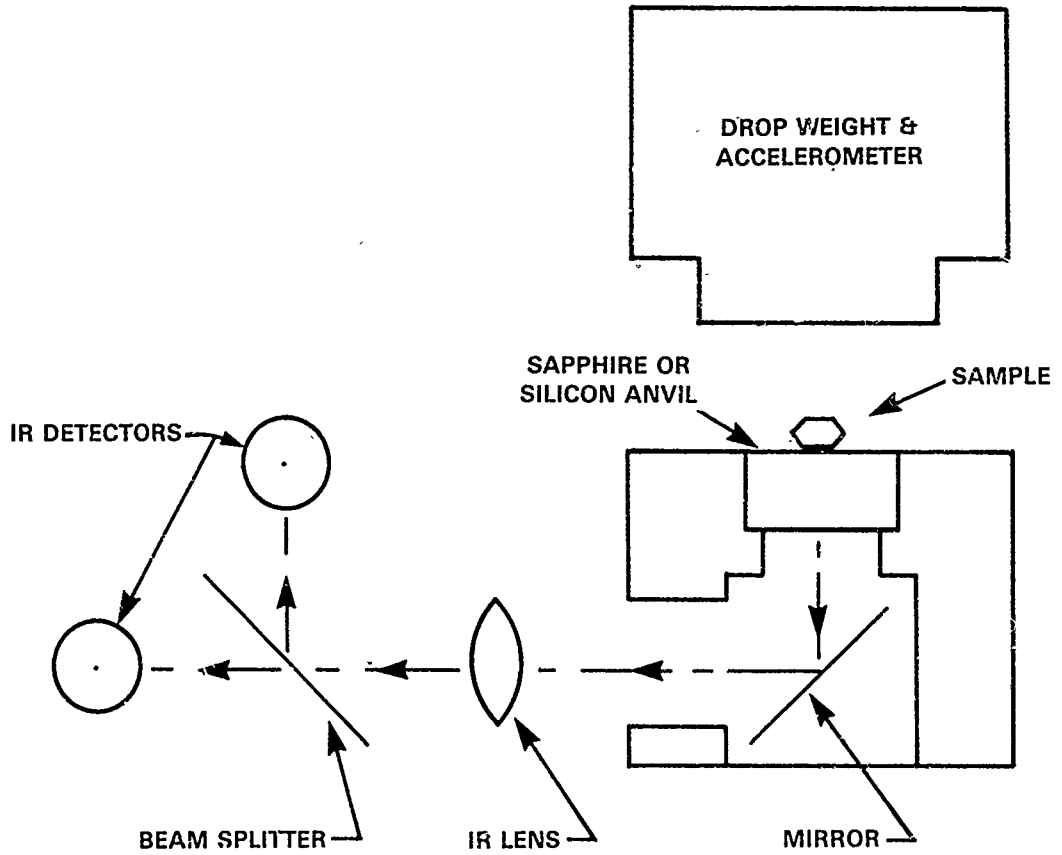


FIGURE 2. SCHEMATIC DRAWING OF ANVIL AND OPTICAL COMPONENTS

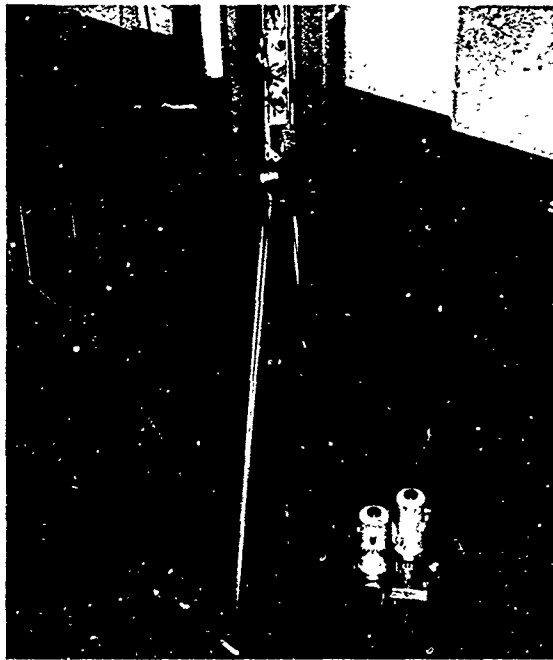


FIGURE 3. IMPACT MACHINE. (INCLUDES GUIDED DROPWEIGHT OF 0.5Kg AND MAXIMUM FREE FALL HEIGHT OF 1.5m AND 5.5m/s VELOCITY. SLINGS INCREASE THE EFFECTIVE HEIGHT TO 20m AND VELOCITY TO 18.5m/sec. THE SAPPHIRE ANVIL AND IR DETECTORS ARE ALSO SHOWN)

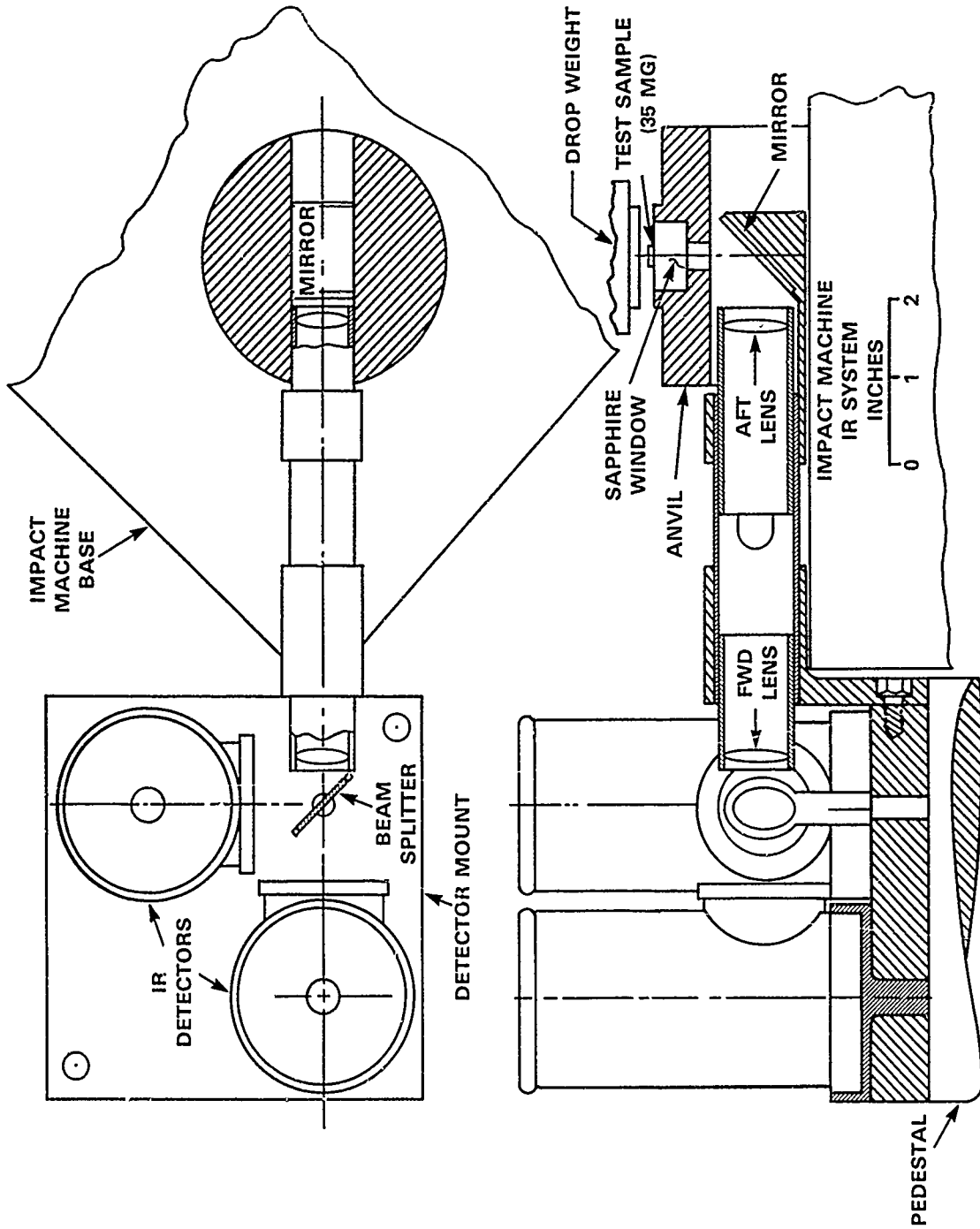


FIGURE 4. DROP TEST ANVIL

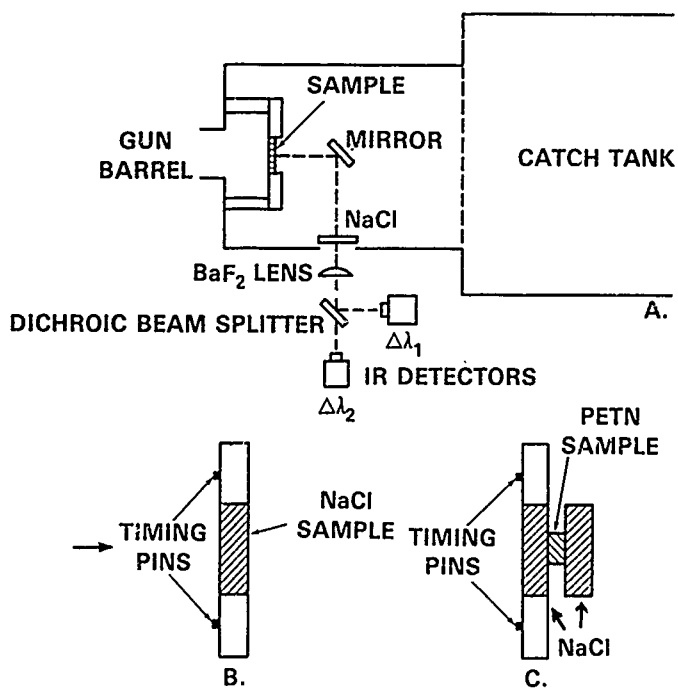


FIGURE 5. SCHEMATIC DIAGRAM OF GAS GUN EXPERIMENTAL CHAMBER (A) DIAGRAM OF NaCl SINGLE CRYSTAL SAMPLE (B) AND DIAGRAM OF PETN CRYSTAL SAMPLE (C) AS DESCRIBED IN THE TEXT

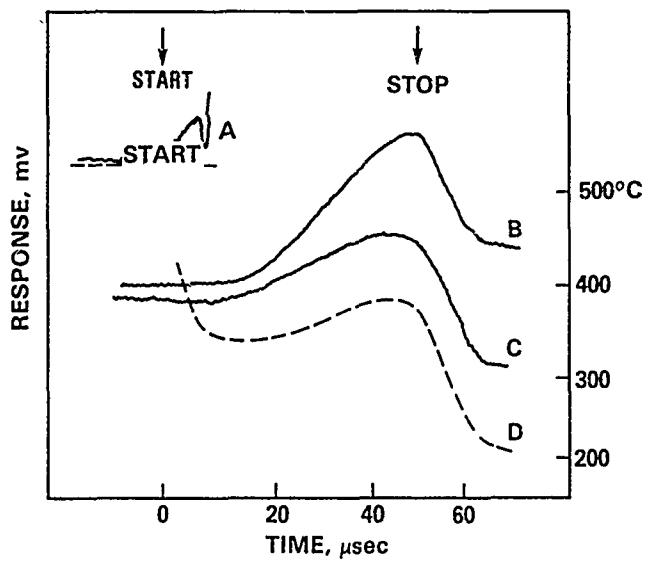


FIGURE 6. INFRARED EMISSION DATA AND TWO-COLOR TEMPERATURE OF NaCl DUE TO 18.5m/sec IMPACT. (CURVE (A) IS THE ACCELEROMETER RESPONSE, (B) AND (C) RESPECTIVELY ARE THE $>5.5 \mu\text{m}$ AND $<5.5 \mu\text{m}$ DETECTOR RESPONSES, AND (D) IS THE CALCULATED TEMPERATURE)

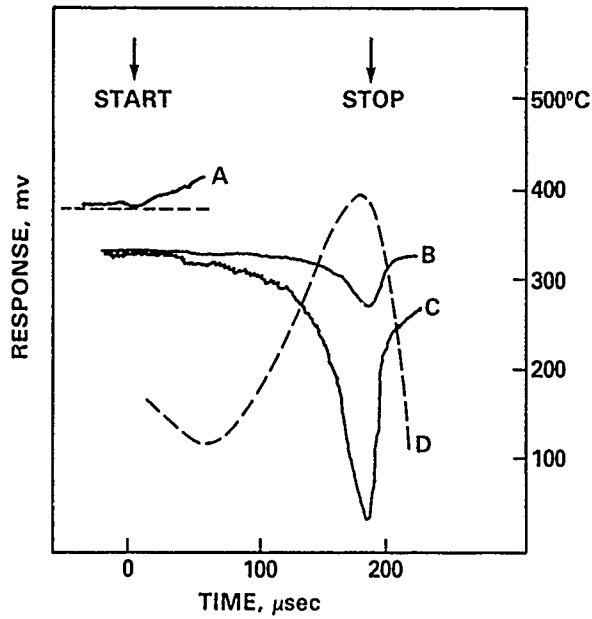


FIGURE 7. INFRARED EMISSION DATA AND TWO-COLOR TEMPERATURE OF AP DUE TO 5.5m/sec IMPACT. (CURVE (A) IS THE ACCELEROMETER RESPONSE (B) AND (C) RESPECTIVELY ARE THE $>5.5\mu\text{m}$ AND $<5.5\mu\text{m}$ DETECTOR RESPONSES, AND (D) IS THE CALCULATED TEMPERATURE)

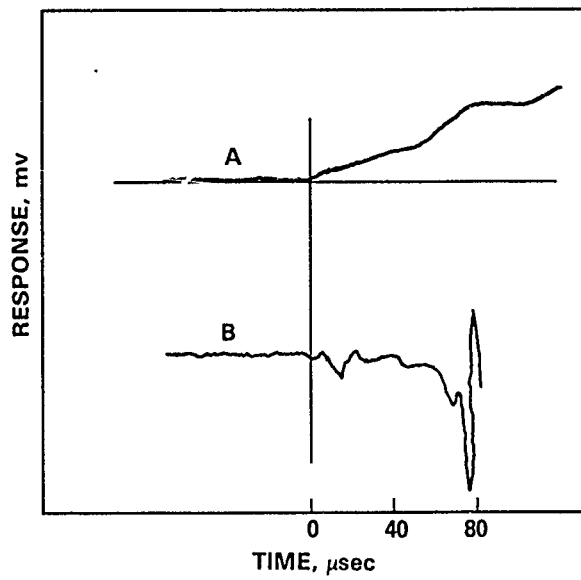


FIGURE 8. INFRARED EMISSION (A) AND ACCELEROMETER RESPONSE (B) OF RDX IMPACTED WITH 5.5m/sec. VELOCITY

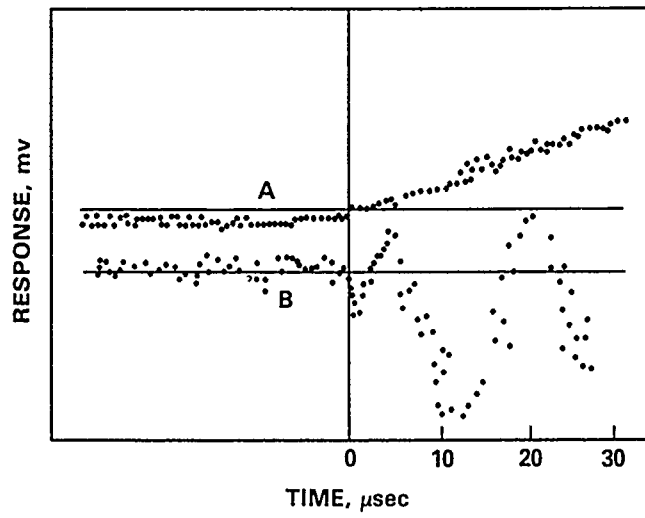


FIGURE 9. INFRARED EMISSION (A) AND ACCELEROMETER RESPONSE (B) OF PETN IMPACTED AT 5.5m/sec. VELOCITY

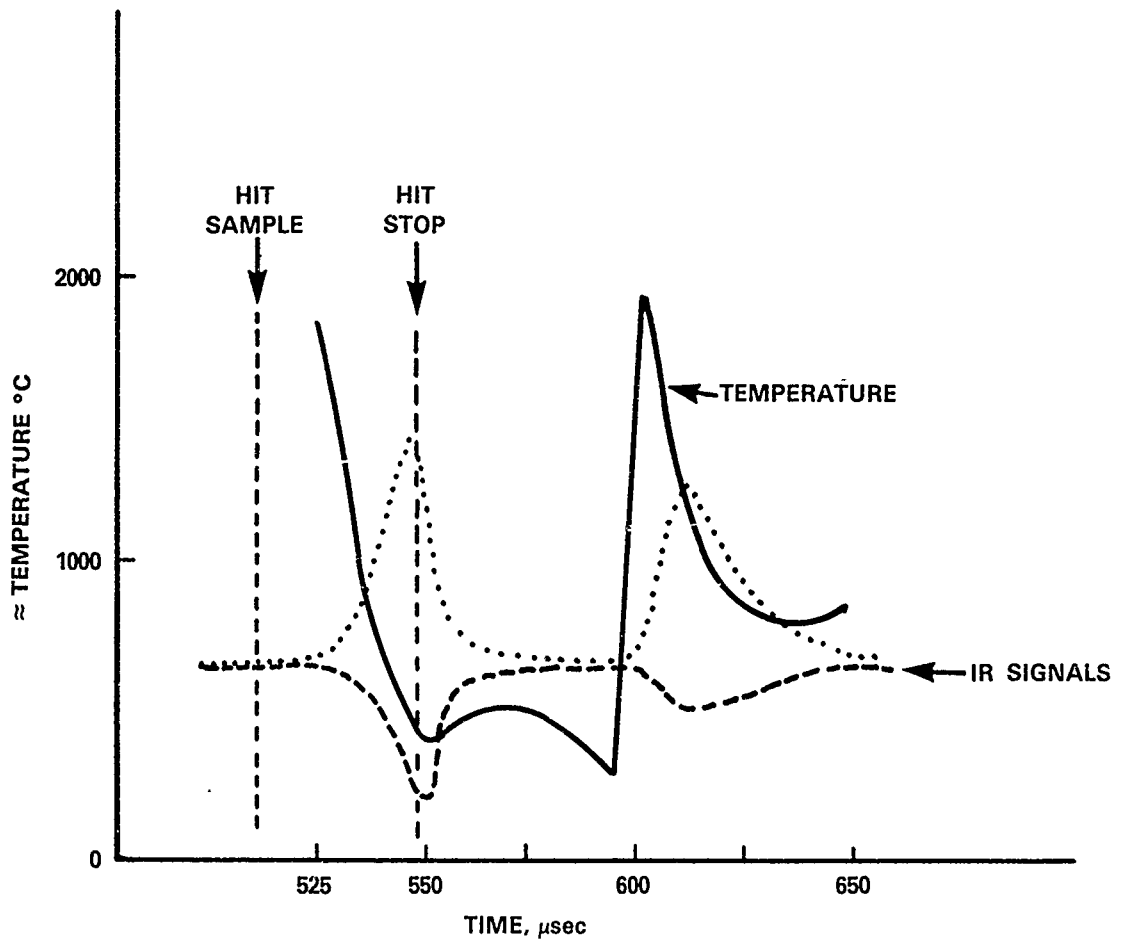


FIGURE 10. PBXN-103 IMPACTED AT 19m/sec. IR RESPONSE AND CALCULATED (IGNITION) TEMPERATURES

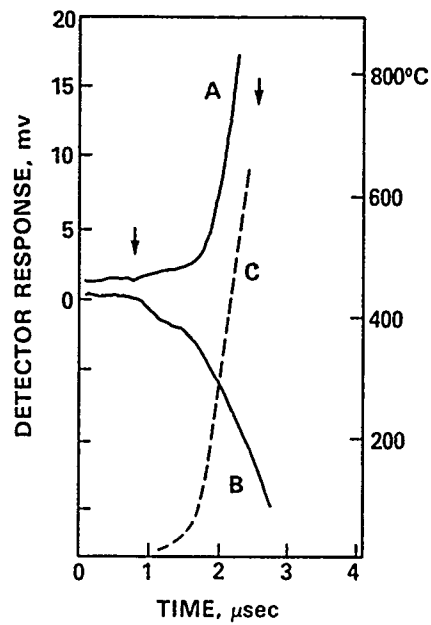


FIGURE 11. INFRARED EMISSION (A) $>5.5\mu\text{m}$ AND (B) $<5.5\mu\text{m}$ AND CALCULATED TWO-COLOR TEMPERATURE (C) OF SINGLE CRYSTAL NaCl IMPACTED AT 485 m/sec. (THE ARROWS SHOW THE ESTIMATED SHOCK ARRIVAL AND EXIT TIMES THROUGH THE SAMPLE)

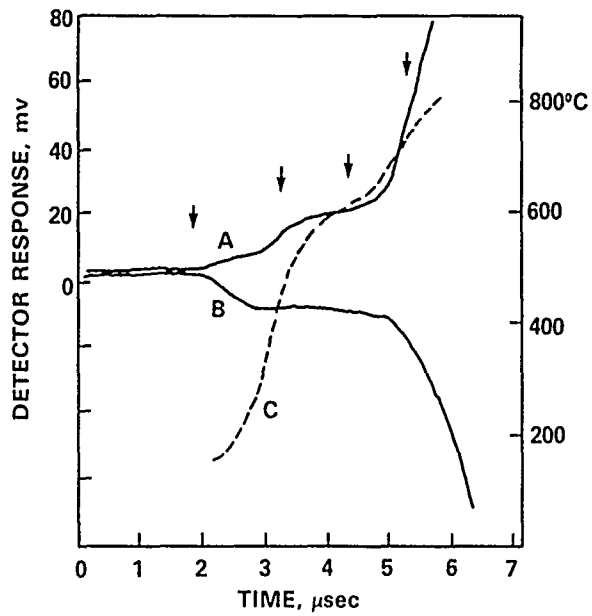
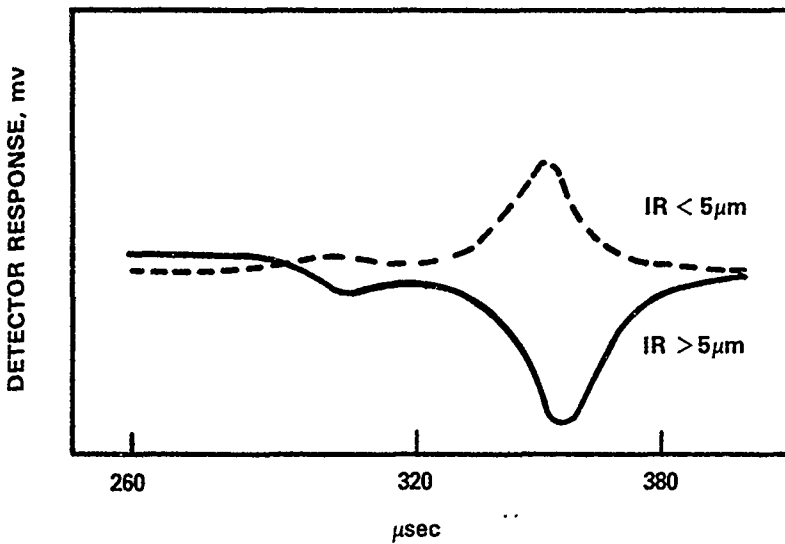


FIGURE 12. INFRARED EMISSION (A) $>5.5\mu\text{m}$ AND (B) $<5.5\mu\text{m}$ AND CALCULATED TWO-COLOR TEMPERATURE (C) OF PETN SINGLE CRYSTAL SANDWICHED BETWEEN TWO NaCl CRYSTALS. (THE ARROWS SHOW THE ESTIMATED ARRIVAL AND EXIT TIMES OF THE SHOCK THROUGH THE SAMPLE COMPONENTS)

A. IR DETECTOR RESPONSES



B. CALCULATED TWO-COLOR TEMPERATURE

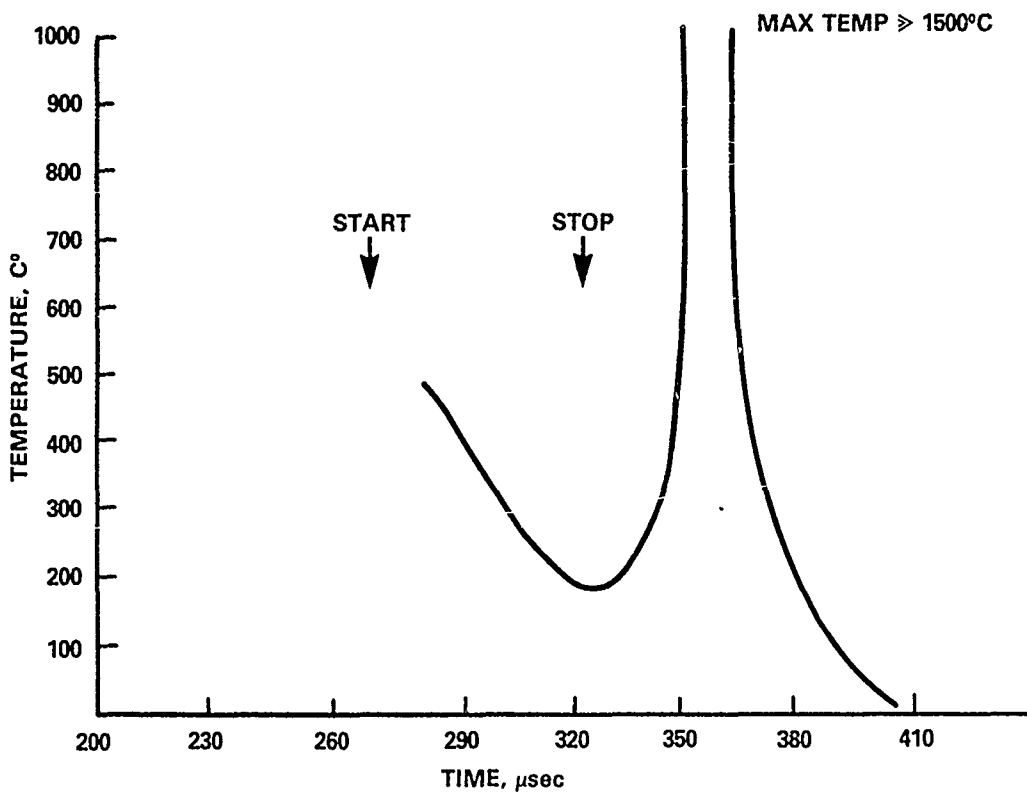


FIGURE 13. AMMONIUM PERCHLORATE IGNITED AT 18m/sec IMPACT (SINGLE CRYSTAL)

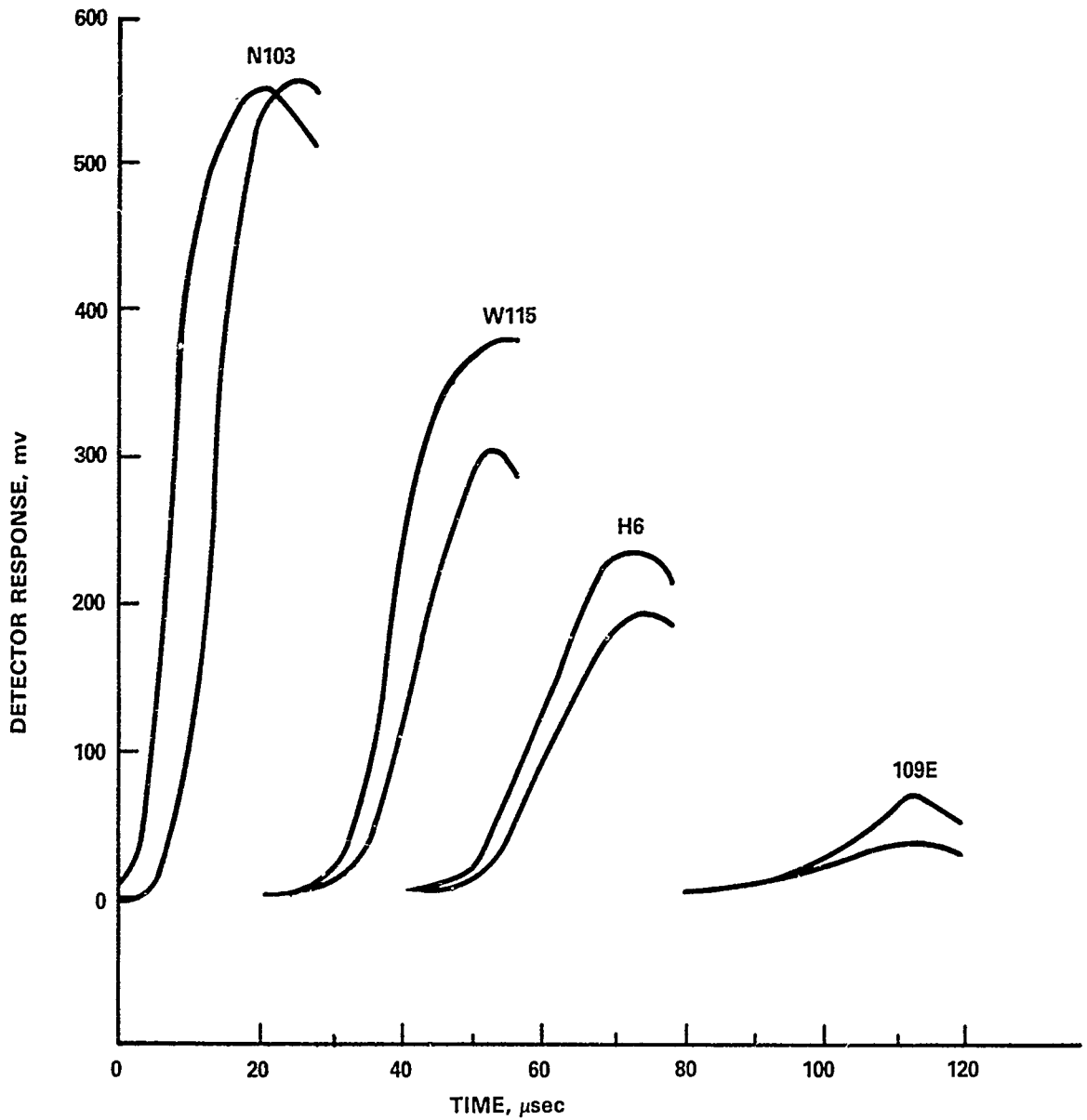


FIGURE 14. INFRARED EMISSION DATA FROM A SERIES OF PBX's IMPACTED AT 17.5m/sec ON SAND

TABLE 1. COMPARISON OF IR EMISSION RATES AND ESTIMATED REACTION RATES FOR SEVERAL EXPLOSIVES

	17 m/sec (on sand)	5.5 m/sec (on sand)	5.5 m/sec (bare tools)	
	<u>Emission rate</u>	<u>Reaction rate**</u>	<u>Emission rate</u>	
		<u>Reaction rate</u>	<u>Emission rate</u>	
			<u>Reaction rate</u>	
PBXN-103	62 mv/μsec	1.2 mg/μsec*	~1 mv/μsec	0.12 mg/μsec
PBXW-115(Q)	28 mv/μsec	0.62 mg/μsec	-	-
H6	11 mv/μsec	0.32 mg/μsec	2.4 mv/μsec	-
PBXW-109(Q)	1.8 mv/μsec	0.10 mg/μsec	-	-

NSWC TR 85-452

*±30% variation with 8 samples.

**Reaction rate estimated by comparing 2-color temperatures to brightness temps to give fraction of sample reacted (assuming that the surface fraction reacted is equivalent to the volume fraction reacted) calculated from the steepest portion of the emission rate curves. (Reference 3)

REFERENCES

1. King, P. J., Catgrove, D. F., and Slate, P. M. B., Behaviors of Dense Media Under High Dynamic Pressures, New York: Gordon and Breach, 1968, p. 513.
2. Raikes, S. A. and Ahrens, T. J., 6th AIRAPT Conference, Jul 1977, Boulder, CO.
3. Von Holle, W. and Trimble, J., Measurement of Post-Shock Temperatures, J. Appl. Phys., 47, 1976 p. 2391.
4. Von Holle, W. and Trimble, J., Temperature Measurement of Shocked Explosives by Time-Resolved Infrared Radiometry - A New Technique to Measure Shock-Induced Reactions, Sixth Symposium (International) on Detonation, Office of Naval Research, Aug 24-27, 1976, p. 691.
5. Von Holle, W. and Tarver, C. M., Temperature Measurement of Shock Heated Solid Explosives by Time Resolved Infrared Radiometry, Seventh Symposium (International) on Detonation, Office of Naval Research, Jun 16-19, 1981, p. 993.
6. Von Holle, W. and Lee, E. L., Measurement of Shock Induced Reaction in Rocket Propellants by Nanosecond Infrared Radiometry and Photography, in Behavior of Dense Media Under High Dynamic Pressures, (Paris Commissariat a l'Energie Atomique, Paris, 1978), p. 425.
7. Coffey, C. S. and DeVost, V. F., Evaluation of Equipment Used to Impact Test Small-Scale Explosive and Propellant Samples, NSWC TR 81-125, Nov 1981.
8. Von Holle, W., Shock Waves in Condensed Matter - 1981 (edited by Nellis, W. J., Seaman, L., and Graham, R. A.) American Institute of Physics Conference Proceedings No. 78, Menlo Park, CA, 1981, p. 287.

DISTRIBUTION

	<u>Copies</u>		<u>Copies</u>
Defense Technical Information Center Cameron Station Alexandria, VA 22314	2	Commander Air Force Armament Laboratory Attn: AFATL/MNE, T. L. Floyd AFATL/MNE, G. Parsons AFATL/DLJ, M. Zimmer Eglin AFB, FL 32542	1 1 1
Commander Naval Sea Systems Command Attn: SEA-662, Dr. R. Bowen SEA-62D31, R. Cassel Washington, DC 20361	1 1	Director Ballistics Research Laboratory Attn: DRCDE-DF, P. Howe Aberdeen Proving Ground Aberdeen, MD 21005	1
Commander Naval Air Systems Command Attn: AIR-54111A Washington, DC 20361	1	Commanding Officer HQ, USAMPBNA Attn: SAR-PBM, T. Sachar Dover, NJ 07801	1
Commander Naval Ordnance Station Attn: PM3A, A. Pereira 2031F, A. Metzner Indian Head, MD 20640	1 1	3C Systems, Inc. Attn: M. Kornhauser 620 Argyle Road Wynnewood, PA 19096	1
Commander Naval Weapons Center Attn: Code 3205, J. Bryant Code 389, T. Boggs Code 326B, G. Greene Code 3266, D. Lind Code 3265, R. Huffman Code 326, M. McCubbin China Lake, CA 93555	1 1 1 1 1 1	Lawrence Livermore National Laboratory Attn: H. Kruger M. Finger B. Hayes E. Lee R. McGuire B. von Holle Technical Library University of California Livermore, CA 94550	1 1 1 1 1 1 1
Commander Naval Weapons Station Attn: Code 50, L. Rothstein Code 503, J. Carlson Code 502, L. Ely Yorktown, VA 23691	1 1 1		

DISTRIBUTION.(Cont.)

	<u>Copies</u>	<u>Internal Distribution:</u>	<u>Copies</u>
Chairman			
DOD Explosives Safety Board			
Attn: J. Ward	1	G12	1
2461 Eisenhower Avenue		G13 (D. Dickinson)	1
Alexandria, VA 22331		H14	1
		R10	1
Office of Naval Research		R10B	1
Attn: ONR-1132P, R. Miller	1	R10C	1
800 North Quincy Street		R10D	1
Arlington, VA 22217		R10F	1
		R10H	1
Office of Naval Technology		R11	1
Attn: ONT-232, D. Houser	1	R11 (E. Anderson)	1
800 North Quincy Street		(C. Gotzmer)	1
Arlington, VA 22217		(J. Leahy)	1
		(L. Burke)	1
Commanding Officer		R12	1
U.S. Army Laboratory Command		R12 (J. Corney)	1
Attn: AMSLC-TD, R. Vitali	1	(O. Dengel)	1
2800 Powder Mill Road		(L. Montesi)	1
Adelphi, MD 20783-1145		R13	3
		R13 (R. Bardo)	1
Commanding Officer		(R. Bernecker)	1
Harry Diamond Laboratories		(A. Clairmont)	1
Attn: DELHD-DE-OM, K. Warner	1	(C. Coffey)	1
2800 Powder Mill Road		(D. Demske)	1
Adelphi, MD 20783-1145		(C. Dickinson)	1
		(J. Forbes)	1
Los Alamos National Laboratory		(R. Granholm)	1
Attn: H. Cady	1	(B. Glancy)	1
J. Dienes	1	(H. Jones)	1
R. Rogers	1	(K. Kim)	1
L. Stretz	1	(R. Lee)	1
Technical Library	1	(R. Lemar)	1
Los Alamos, NM 87544		(P. Miller)	1
		(C. Richmond)	1
Sandia National Laboratory		(H. Sandusky)	1
Attn: J. Asay	1	(G. Sutherland)	1
R. Graham	1	(D. Tasker)	1
Albuquerque, NM 37115		(J. Watt)	1
		(F. Zerilli)	1

DISTRIBUTION (Cont.)

Internal Distribution:

	<u>Copies</u>
R14	1
R14 (T. Farley)	1
(J. Gaspin)	1
R15	1
R15 (D. Houchins)	1
R16	1
R16 (E. Kayser)	1
(A. Tompa)	1
E231	15
E232	3